RESEARCH ARTICLE

Convergence of Alarmone and Cell Cycle Signaling from *Trans*-Encoded Sensory Domains

Stefano Sanselicio, Patrick H. Viollier

Department of Microbiology and Molecular Medicine, Institute of Genetics and Genomics in Geneva (iGE3), Faculty of Medicine, University of Geneva, Geneva, Switzerland

ABSTRACT **Despite the myriad of different sensory domains encoded in bacterial genomes, only a few are known to control the cell cycle. Here, suppressor genetics was used to unveil the regulatory interplay between the PAS (Per-Arnt-Sim) domain protein MopJ and the uncharacterized GAF (cyclic GMP-phosphodiesterase–adenylyl cyclase–FhlA) domain protein PtsP, which resembles an alternative component of the phosphoenolpyruvate (PEP) transferase system. Both of these systems indirectly target the *Caulobacter crescentus* cell cycle master regulator CtrA, but in different ways. While MopJ acts on CtrA via the cell cycle kinases DivJ and DivL, which control the removal of CtrA at the G_1-S transition, our data show that PtsP signals through the conserved alarmone (p)ppGpp, which prevents CtrA cycling under nutritional stress and in stationary phase. We found that PtsP interacts genetically and physically with the (p)ppGpp synthase/hydrolase SpoT and that it modulates several promoters that are directly activated by the cell cycle transcriptional regulator GcrA. Thus, parallel systems integrate nutritional and systemic signals within the cell cycle transcriptional network, converging on the essential alphaproteobacterial regulator CtrA while also affecting global cell cycle transcription in other ways.**

IMPORTANCE **Many alphaproteobacteria divide asymmetrically, and their cell cycle progression is carefully regulated. How these bacteria control the cell cycle in response to nutrient limitation is not well understood. Here, we identify a multicomponent signaling pathway that acts on the cell cycle when nutrients become scarce in stationary phase. We show that efficient accumulation of the master cell cycle regulator CtrA in stationary-phase *Caulobacter crescentus* cells requires the previously identified stationary-phase/cell cycle regulator MopJ as well as the phosphoenolpyruvate protein phosphotransferase PtsP, which acts via the conserved (p)ppGpp synthase SpoT. We identify cell cycle-regulated promoters that are affected by this pathway, providing an explanation of how (p)ppGpp-signaling might couple starvation to control cell cycle progression in *Caulobacter* spp. and likely other *Alphaproteobacteria*. This pathway has the potential to integrate carbon fluctuation into cell cycle control, since in phosphotransferase systems it is the glycolytic product phosphenolpyruvate (PEP) rather than ATP that is used as the phosphor donor for phosphorylation.**

Received 18 August 2015 **Accepted** 23 September 2015 **Published** 20 October 2015

Citation Sanselicio S, Viollier PH. 2015. Convergence of alarmone and cell cycle signaling from *trans*-encoded sensory domains. mBio 6(5):e01415-15. doi:10.1128/mBio.01415-15.

Editor Vanessa Sperandio, UT Southwestern Medical Center Dallas

Address correspondence to Patrick H. Viollier, patrick.viollier@unige.ch.

Cellular motility is responsive to external signals, such as nutritional changes, but it is also regulated by cues that occur systemically during each cell division cycle (1, 2). The latter characteristic has been successfully exploited in forward genetic screens that employ motility as a proxy to unearth mutations in cell cycle regulators in the synchronizable alphaproteobacterium *Caulobacter crescentus* (here, *C. crescentus*) (3, 4). Motility is conferred by a single polar flagellum that drives the dispersal of *C. crescentus* swarmer cells. Swarmer cells harbor a flagellum and several adhesive pili at the old cell pole, while residing in a replication-incompetent state resembling the eukaryotic G_1 phase. These G_1-phase-like swarmer cells emerge from an asymmetric division that spawns a swarmer cell and a replicative stalked cell at each division. The latter bears a cylindrical extension of the cell envelope (the stalk) tipped by an adhesive holdfast at the old cell pole (Fig. 1A) and resides in S phase (2). During the G_1-S transition, the swarmer cell morphs into a stalked cell that initiates DNA replication.

CtrA, a DNA-binding response regulator (RR) of the OmpR family (3), controls the coordination of the cell cycle and polar morphogenesis at the transcriptional level. CtrA not only directly activates promoters of flagellar, pilus, holdfast, and cell division genes (5–7), but it also acts as a negative regulator of gene expression and, directly and/or indirectly, the initiation step of DNA replication by restricting firing at the origin of replication (*Cori*) (8, 9). DNA replication initiates only once during the *C. crescentus* cell cycle, and CtrA's activity is precisely regulated to permit coordination of transcription with the replication cycle (10).

As for most RRs, the DNA-binding activity of CtrA is regulated by phosphorylation at a conserved aspartate (Asp) residue (3, 10). This phosphorylation step is generally executed by a histidine kinase (HK) that upon dimerization first *trans*-autophosphorylates

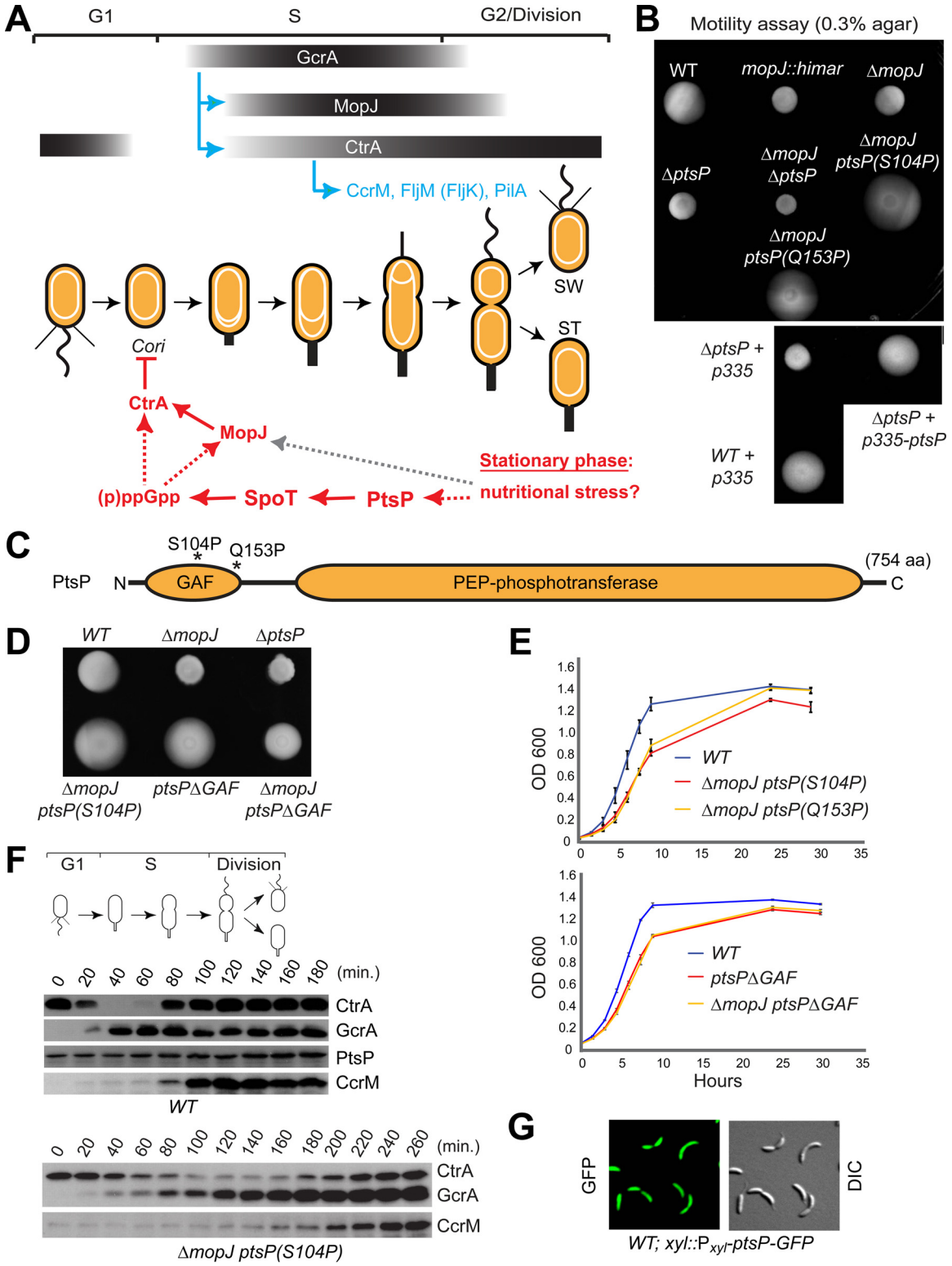

FIG 1 MopJ and PtsP are pleiotropic regulators that control motility and cell cycle progression in *Caulobacter crescentus*. (A) Model showing the *C. crescentus* cell cycle and the relevant cell cycle transcriptional regulators CtrA and GcrA, as well as the recently described single PAS domain protein MopJ (23). The thin black vertical line represents the flagellar filament (composed of FljK, FljM, and other flagellins), before it rotates (wavy line). The thick vertical black line represents the stalk, and the white oval represents the chromosome, whose replication is initiated at the *C. crescentus* origin of replication (*Cori*). The thin slanted black lines represent the polar pili (composed of the PilA pilin). The expression of MopJ and CtrA is transcriptionally activated by GcrA (blue arrows), while CtrA activates expression of the methylase CcrM, the flagellin FljM, and the pilin PilA. Expression of the flagellin FljK by CtrA is indirect (7). Shown underneath is a model of the (p)ppGpp-dependent signaling pathways in stationary-phase *C. crescentus* cells described in the text. Dashed arrows indicate connections that are poorly defined. (B, top) Motility assay on swarm (0.3%) agar for WT, *mopJ*::*himar*, Δ*mopJ*, and Δ*ptsP* single mutants, the Δ*mopJ* Δ*ptsP* double mutant, and two

(Continued)

on a conserved histidine (His) in an ATP-dependent manner (11). However, phosphorylation of CtrA underlies a multicomponent His-Asp (HA) relay, regulated in time and space (12) to restrict CtrA activity and its presence during the cell cycle. CtrA is abundant in G_1 phase, degraded at the G_1-S transition, resynthesized in S-phase after transcriptional activation from its promoter by the conserved regulator GcrA (13, 14) (Fig. 1A), and subsequently phosphorylated by the HA relay (3, 10, 12). The degradation of CtrA at the G_1-S transition requires the single-domain RR CpdR (15, 16), which is itself phosphorylated by the same HA relay acting on CtrA. In the absence of CpdR, CtrA protein levels no longer oscillate during the cell cycle (15, 16).

The conserved alarmone (p)ppGpp (guanosine 3′,5′-bispyrophosphate) is induced under different starvation conditions, and in stationary phase it also interferes with CtrA oscillations through an unknown mechanism (17–21). Although conditions of nitrogen or carbon starvation are known to result in the induction of (p)ppGpp via the synthase/hydrolase SpoT in *C. crescentus* (17–20), it is unclear how nutritional changes are perceived and relayed to SpoT to keep cells idling in the (motile) G_1 phase. Interestingly, a nutritional downshift has been used for the enrichment of G_1-phase cells in the related alphaproteobacterium *Sinorhizobium meliloti*, suggesting that (p)ppGpp acts in a comparable manner in related systems (22).

Since the fraction of G_1-phase cells within a population defines the overall motility of a colony on swarm (0.3%) agar, genetic dissection of the (p)ppGpp signaling pathway may be possible through the analysis of motility mutants. A motility screen in *C. crescentus* conducted on swarm agar led to the recent discovery of the conserved *mopJ* gene as a determinant that promotes the accumulation of G_1-phase cells and CtrA in stationary phase (23). It encodes a single-domain PAS (Per-Arnt-Sim) protein that targets several polar HA relay components for CtrA. Importantly, the MopJ protein is strongly induced in stationary phase, and (p)ppGpp is necessary for induction of the *mopJ* promoter (P_{mopJ}) in stationary phase and sufficient for induction in exponential phase (23).

The PAS and the related GAF (cyclic GMP-phosphodiesterase–adenylyl cyclase–FhlA) domains perceive metabolic or energetic changes from within the environment or within cells and transduce these signals into adaptive responses, often by binding small-molecule ligands, and are frequently encoded on the same polypeptide (24). Here, we report gain-of-function mutations in the GAF domain of the phosphoenolpyruvate protein phosphotransferase PtsP; these mutations were identified as motility suppressors of *mopJ* null mutants (Δ*mopJ*). We show that these suppressor mutations act by restoring accumulation of CtrA in stationary-phase Δ*mopJ* cells, and we provide evidence that PtsP signals via SpoT. Intriguingly, this signaling pathway also appears to enhance the activity of promoters that are direct targets of the S-phase transcriptional regulator GcrA, including the promoter of *ctrA*. The convergence of PAS and GAF domain signaling pathways on the conserved master regulator CtrA illustrates the plasticity of the regulatory network controlling alphaproteobacterial cell cycle progression in different phases of growth.

RESULTS

Mutations in the GAF domain of PtsP suppress the motility defect of Δ*mopJ* cells. Prolonged incubation of Δ*mopJ* colonies on swarm agar gives rise to highly motile flares growing out from the poorly motile Δ*mopJ* background (23). Whole-genome sequencing of two such Δ*mopJ* motility suppressors (Fig. 1B) revealed a single missense mutation (S104P or Q153P) in the GAF domain-encoding region of PtsP (CCNA_00892) (Fig. 1C) in each strain. PtsP resembles E1 regulatory components of the phosphoenolpyruvate (PEP)-dependent transport system (PTS) that typically use PEP rather than ATP as the phospho donor to phosphorylate client proteins such as the Hpr phospho-carrier protein (25).

We investigated the role of PtsP in motility by constructing an in-frame deletion in *ptsP* (Δ*ptsP*) in wild-type (WT; NA1000) cells, and we observed a reduction in motility on swarm agar (Fig. 1B) that was restored by complementation with a plasmid carrying *ptsP* (pMT335-*ptsP*) (Fig. 1B). Flow cytometry (Fig. 2A and B) and differential interference contrast (DIC) microscopy (Fig. 2C and D) additionally revealed that the Δ*ptsP* mutation reduced the number of G_1-phase cells in the exponential and stationary phases and caused a mild perturbation in cytokinesis, akin to that observed with the Δ*mopJ* strain (Fig. 1B and 2A to D) (23). The Δ*ptsP* mutation accentuated the defects of the Δ*mopJ* strain (Fig. 1B and 2A to D), indicating that MopJ and PtsP control similar functions.

Since the Δ*ptsP* mutation impaired swarming motility, while the *ptsP*(S104P) and *ptsP*(Q153P) constructs appeared to enhance it by way of a replacement of a polar residue with a secondary structure-breaking proline, we reasoned that the GAF^{S104P} and GAF^{Q153P} mutations might confer a gain-of-function mutation to PtsP. To test this idea, we deleted the GAF-encoding residues (residues 33 to 159) of *ptsP* from WT and Δ*mopJ* cells to determine if the GAF domain simply acts as an autoinhibitory domain. Using swarming motility as readout (Fig. 1D), we observed that the resulting *ptsP*Δ*GAF* single mutant and the Δ*mopJ ptsP*Δ*GAF* double mutant exhibited a slight increase in motility compared to their parental strains on swarm agar. We also observed that the growth rates of the Δ*mopJ ptsP*Δ*GAF* double mutant and the *ptsP*Δ*GAF* single mutant were diminished compared to the WT, akin to the Δ*mopJ ptsP*(S104P) and Δ*mopJ ptsP*(Q153P) strains (Fig. 1E), supporting the notion that the Δ*GAF* mutation can relieve autoinhibition or at least partially phenocopy the point mutations. In

Figure Legend Continued

spontaneously isolated Δ*mopJ* motility suppressors, Δ*mopJ ptsP*(S104P) and Δ*mopJ ptsP*(Q153P). (Bottom) Complementation of the Δ*ptsP* motility defect with pMT335-*ptsP* (p335-*ptsP*), but not with empty pMT335 (p335). WT cells harboring empty pMT335 (p335) are also shown. (C) Domain organization of PtsP from the N to C terminus, indicating the total length in amino acids (aa) of the protein. Asterisks inidcate the position of the suppressive mutation in the PtsP GAF domain. (D) Motility assay on soft (0.3%) agar with WT, Δ*mopJ*, Δ*ptsP*, Δ*mopJ ptsP*(S104P), *ptsP*Δ*GAF*, and Δ*mopJ ptsP*Δ*GAF* strains. (E) The *ptsP*(S104P) or *ptsP*(Q153P) suppressor mutations in Δ*mopJ* (top) and the deletion of the GAF domain of *ptsP* in the WT or in the Δ*mopJ* background (bottom) increased the doubling time of cells. Growth curves are shown for the WT, Δ*mopJ ptsP*(S104P), Δ*mopJ ptsP*(Q153P), *ptsP*Δ*GAF*, and Δ*mopJ ptsP*Δ*GAF* cells in PYE. Error bars in the graph indicate standard deviations. (F) Immunoblot showing the steady-state levels of PtsP, CtrA, GcrA, and CcrM during the cell cycle of WT cells (top) or Δ*mopJ ptsP*(S104P) cells (bottom). The time (in minutes) after synchronization is indicated above the blots. (G) Fluorescence and DIC images show the localization pattern of PtsP-GFP (C-terminal fusion of PtsP to GFP) expressed under the control of P_{xyl} (xylose inducible) at the *xylX* locus in WT cells.

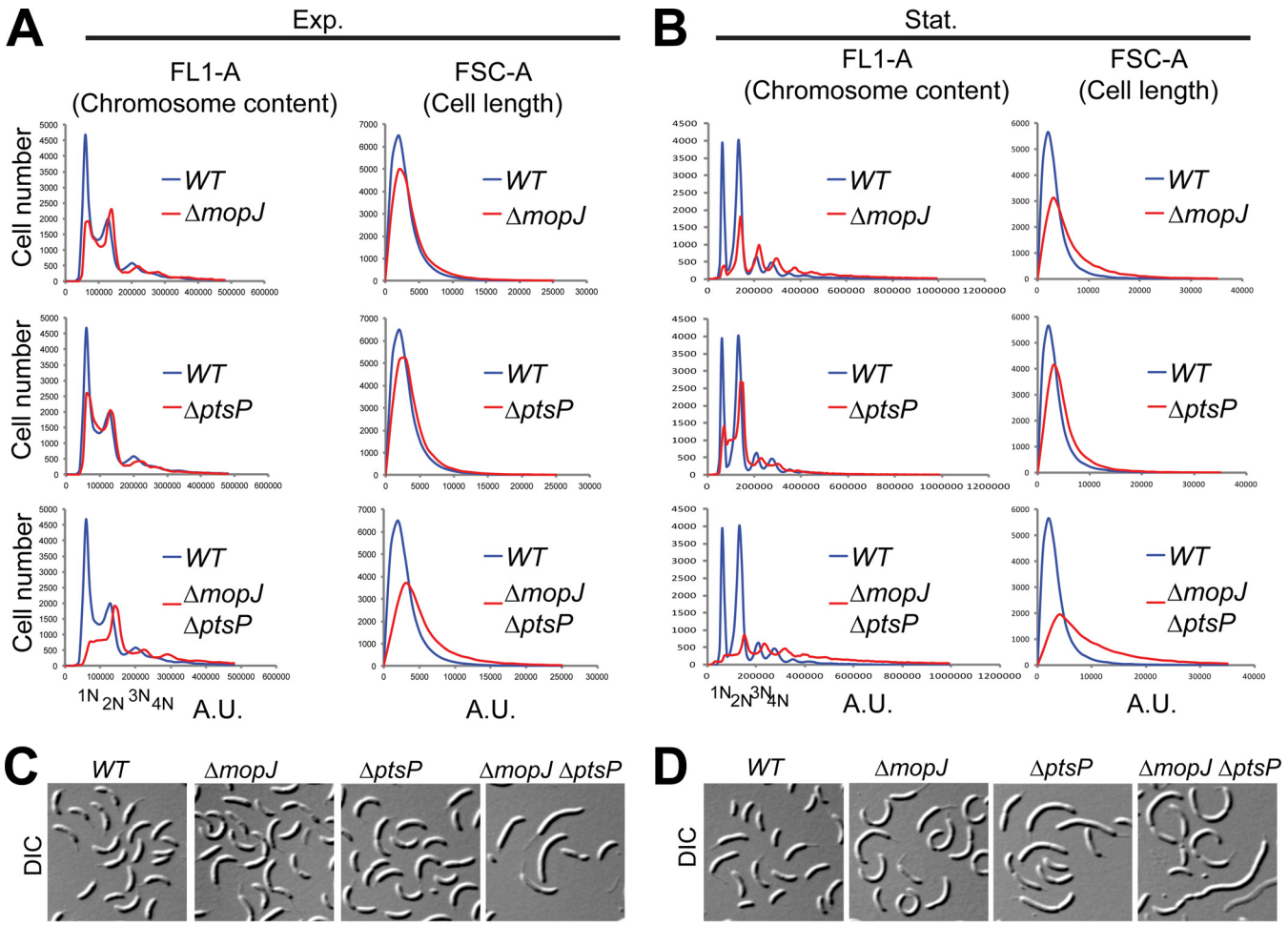

FIG 2 MopJ and PtsP promote the accumulation of G_1-phase cells. (A and B) FACS analysis of Δ*mopJ* and Δ*ptsP* mutant strains and the Δ*mopJ* Δ*ptsP* double mutant strain showed a reduction in G_1 phase. Genome content (FL1-A channel) and cell size (FSC-A channel) were analyzed by FACS during exponential (A) and stationary (B) phases in M2G. (C and D) Δ*mopJ* and Δ*ptsP* single mutants and the Δ*mopJ* Δ*ptsP* double mutant showed filamentation. DIC images of WT, Δ*mopJ* and Δ*ptsP* single mutants, and the Δ*mopJ* Δ*ptsP* double mutant during exponential (C) and stationary (D) growth phases in M2G.

contrast, the growth rates of the Δ*mopJ* and Δ*ptsP* single mutants were similar to that of the WT (see Fig. S1 in the supplemental material).

PtsP affects CtrA accumulation in stationary phase and during the cell cycle. To explore the possibility that the reduced growth rate of the Δ*mopJ ptsP*(S104P) mutant (the mutant exhibiting the lowest growth rate) stems from a deregulated cell cycle, we conducted immunoblotting experiments using antibodies against CtrA, GcrA, and the DNA methyltransferase CcrM, whose gene is directly regulated by CtrA (Fig. 1A), in synchronized cells. We observed that the cycling of CtrA and CcrM was altered in the Δ*mopJ ptsP*(S104P) strain versus the WT, while the appearance of GcrA seemed not affected or only mildly affected (Fig. 1F). Difficulties in obtaining a stable *mopJ*$^+$ *ptsP*(S104P) strain prevented us from exploring if this mutation in isolation also affects the cell cycle.

The altered cycling of CtrA and CcrM in Δ*mopJ ptsP*(S104P) cells prompted us to assay the CtrA-activated pP_{pilA}-*lacZ*, pP_{sciP}-*lacZ*, pP_{fljM}-*lacZ*, and pP_{fljK}-*lacZ* promoter-probe plasmids (note that P_{fljK} is indirectly activated by CtrA, while the others are directly activated) in exponential-phase (Fig. 3A) and stationary-phase (Fig. 3B) *ptsP* and *mopJ* single and double mutant cells. We observed a commensurate reduction in promoter activity in the Δ*mopJ* Δ*ptsP* double mutant compared to the Δ*ptsP* and Δ*mopJ* single mutants, with the strongest effect occurring in stationary phase (Fig. 3B). In contrast, in the Δ*mopJ ptsP*(S104P) and Δ*mopJ ptsP*(Q153P) suppressor mutants, there was a strong upregulation of LacZ activity relative to the WT (Fig. 3A and B). Immunoblotting using polyclonal antibodies against FljK, SciP, and PilA confirmed these transcriptional trends of the Δ*mopJ ptsP*(S104P) and Δ*mopJ ptsP*(Q153P) suppressor mutants (Fig. 3C and D). (Note that the PilA protein is absent from stationary-phase WT cells for reasons that are currently unknown, but it likely operates at the post-transcriptional level [compare Fig. 3B and D]).

We also observed a strong reduction in CtrA steady-state levels in stationary-phase Δ*ptsP* cells, similar to the response of Δ*mopJ* cells observed previously (Fig. 3E) (23). This effect was not apparent in exponential-phase cells (Fig. 3E), and only a weak effect was seen during the transition from exponential to stationary phase (see Fig. S2A in the supplemental material). In contrast, CtrA-M2, a version of CtrA that is no longer degraded by the ClpXP protease because the C-terminal proteolytic signal has been masked (10),

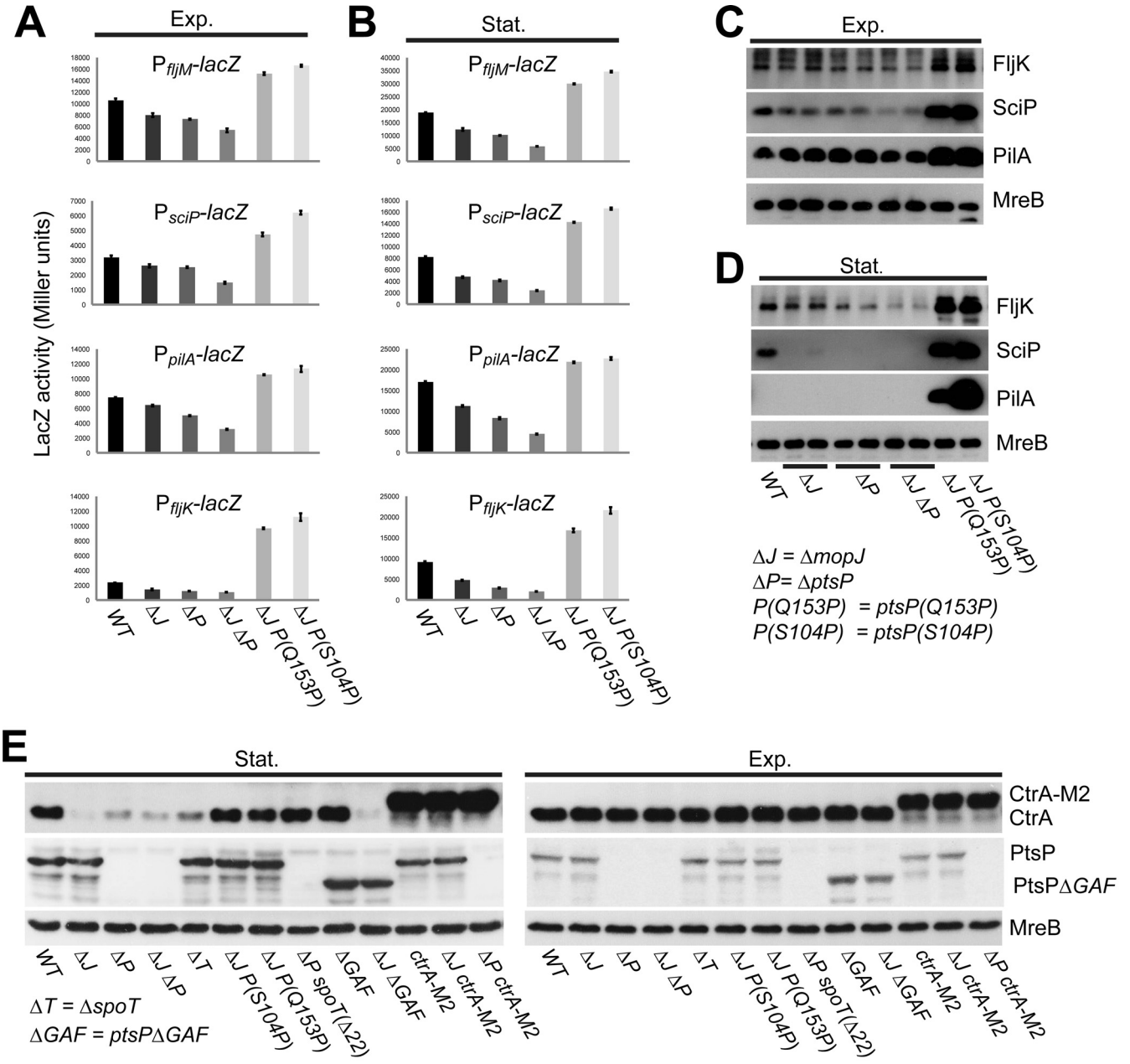
A
Exp.
B
Stat.
C
Exp.
D
Stat.
LacZ activity (Miller units)
P fljM-lacZ
P sciP-lacZ
P pilA-lacZ
P fljK-lacZ
FljK
SciP
PilA
MreB
WT
ΔJ
ΔP
ΔJ ΔP
ΔJ P(Q153P)
ΔJ P(S104P)
ΔJ = ΔmopJ
ΔP= ΔptsP
P(Q153P) = ptsP(Q153P)
P(S104P) = ptsP(S104P)

E
Stat.
Exp.
CtrA-M2
CtrA
PtsP
PtsPΔGAF
MreB
WT
ΔJ
ΔP
ΔJ ΔP
ΔT
ΔJ P(S104P)
ΔJ P(Q153P)
ΔP spoT(Δ22)
ΔGAF
ΔJ ΔGAF
ctrA-M2
ΔJ ctrA-M2
ΔP ctrA-M2
ΔT = ΔspoT
ΔGAF = ptsPΔGAF

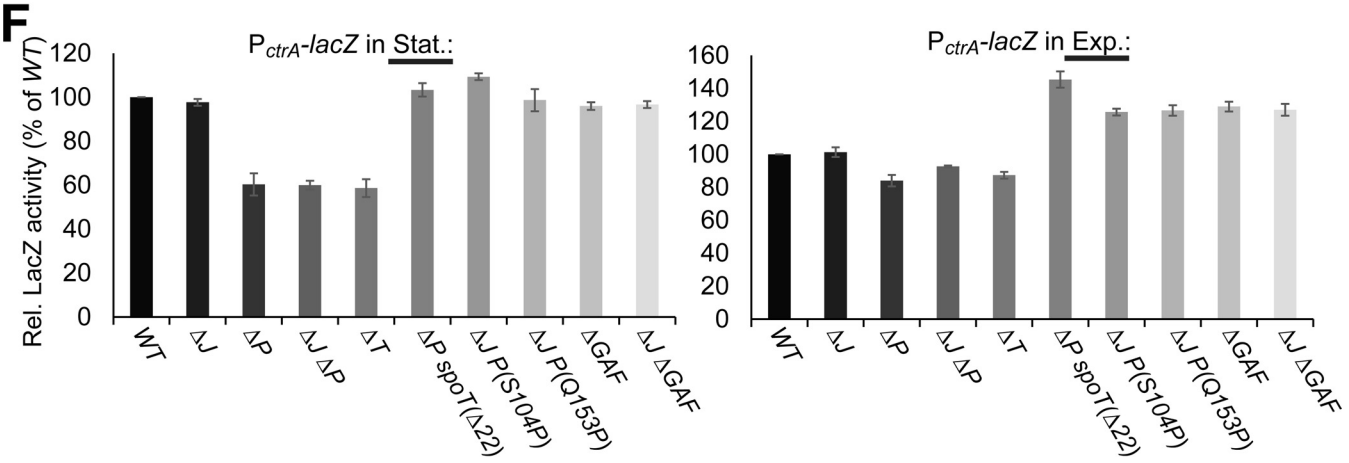
F
Rel. LacZ activity (% of WT)
P ctrA-lacZ in Stat.:
P ctrA-lacZ in Exp.:
WT
ΔJ
ΔP
ΔJ ΔP
ΔT
ΔP spoT(Δ22)
ΔJ P(S104P)
ΔJ P(Q153P)
ΔGAF
ΔJ ΔGAF

accumulates to near-wild-type steady-state levels in stationary-phase Δ*mopJ* or Δ*ptsP* cells (Fig. 3E). CtrA accumulation is similarly restored when the CpdR proteolytic regulator of CtrA is inactivated (15, 16) (see Fig. S2B), indicating that MopJ and PtsP (indirectly) protect CtrA from degradation in stationary phase. In contrast, the steady-state levels of CtrA in stationary Δ*mopJ ptsP*(S104P) and Δ*mopJ ptsP*(S153P) cells were near (or exceeded) WT levels (Fig. 3E), showing that the *ptsP* suppressor mutations act positively on CtrA abundance, at least in the context of a Δ*mopJ* mutation. In support of the idea that *ptsP* mutations additionally affect *ctrA* promoter activity, LacZ measurements (β-galactosidase assays) of strains harboring the pP_{ctrA}-*lacZ* reporter plasmid revealed a strong reduction in stationary Δ*ptsP* and Δ*mopJ* Δ*ptsP* cells, but near-wild-type activity in Δ*mopJ ptsP* (S104P), Δ*mopJ ptsP*(Q153P), and Δ*mopJ ptsP*(Δ*GAF*) mutants (Fig. 3F).

We conclude that MopJ and PtsP influence CtrA at the post-transcriptional level, while PtsP additionally promotes *ctrA* transcription. GcrA and CtrA both positively and directly regulate transcription of the *ctrA* gene via the P1 and the P2 promoter, respectively (13, 14, 26). Thus, our finding that CtrA abundance, but not P_{ctrA}-*lacZ* activity, is reduced in stationary-phase Δ*mopJ* cells (Fig. 3E and F) implies that P_{ctrA} activity can be sustained in a (largely) CtrA-independent manner in stationary phase, perhaps via GcrA or a related pathway (this is explored further below [Fig. 4G; see also Fig. S3C in the supplemental material]).

PtsP signals via SpoT. To further dissect the PtsP signaling pathway genetically, we isolated a motility suppressor of the Δ*ptsP* mutant and found by genome sequencing an in-frame deletion encoding residues 493 to 514 of the C-terminal regulatory domain of the (p)ppGpp synthase/hydrolase SpoT (27) in this strain (Δ*ptsP* $spoT^{\Delta 22}$) (Fig. 4A and B). The $spoT^{\Delta 22}$ mutation also improved the motility of the Δ*ptsP mopJ*::*himar1* double mutant (Fig. 4B; see also Fig. S3A in the supplemental material), although to a lesser extent, possibly because of a contribution of MopJ to motility. Consistent with the notion that the $spoT^{\Delta 22}$ allele is a gain-of-function mutation that causes an ectopic increase in (p)ppGpp levels, induction of (p)ppGpp from the heterologous (p)ppGpp constitutively active synthase RelA′ (which lacks the C-terminal regulatory domain) of *Escherichia coli* (17, 21) is sufficient to improve motility of Δ*ptsP* cells on swarm agar (Fig. 4C), thus acting analogous to the $spoT^{\Delta 22}$ mutation. In contrast, the Δ*spoT* deletion phenocopies the motility of the Δ*ptsP* mutant and the motility of Δ*spoT mopJ*::*himar1* mutant strain resembles that of the Δ*ptsP mopJ*::*himar1* strain (Fig. 4B).

As for the Δ*ptsP* strain, CtrA abundance and P_{ctrA}-*lacZ* activity were strongly reduced in stationary-phase Δ*spoT* cells (Fig. 3E and F). CtrA levels were restored in stationary-phase Δ*ptsP* $spoT^{\Delta 22}$ double mutant cells (Fig. 3E), and P_{ctrA}-*lacZ* activity in exponential- or stationary-phase Δ*ptsP* $spoT^{\Delta 22}$ cells was elevated relative to the WT (Fig. 3F). Moreover, experiments using CtrA-dependent promoter probe plasmids revealed that transcriptional activity in Δ*ptsP* $spoT^{\Delta 22}$ double mutant cells was higher than in the WT (Fig. 4F), unlike the Δ*ptsP* single mutant (Fig. 3B). Lastly, pulldown experiments using epitope-tagged variants of SpoT or PtsP (Fig. 4D and E; see also Fig. S3B in the supplemental material) revealed that both proteins interact directly or indirectly.

PtsP and SpoT act on GcrA target promoters. The difference in motility between the Δ*ptsP* $spoT^{\Delta 22}$ double mutant and the Δ*ptsP* $spoT^{\Delta 22}$ *mopJ*::*himar1* triple mutant strains (Fig. 4B) raised the possibility that MopJ is regulated by the PtsP pathway. Indeed, we previously showed that expression of a transcriptional fusion of the *mopJ* promoter to the *lacZ* reporter gene (P_{mopJ}-*lacZ*) is regulated by (p)ppGpp; artificial induction of (p)ppGpp during exponential growth augmented P_{mopJ}-*lacZ* activity, while it was diminished in stationary-phase Δ*spoT* cells (23). As shown in Fig. 4G, P_{mopJ}-*lacZ* is also downregulated by the Δ*ptsP* deletion to the same extent as by the Δ*spoT* mutation. Conversely, P_{mopJ}-*lacZ* is restored in exponential-phase Δ*ptsP* $spoT^{\Delta 22}$ cells, even exceeding the values for WT cells (Fig. 4G). These results mirrored those obtained with the P_{ctrA}-*lacZ* reporter plasmid, and since P_{mopJ} and P_{ctrA} are both targets of GcrA, we hypothesized that PtsP/SpoT signaling may affect other GcrA target promoters. In support of this idea, we found that the activity of P_{tipF}-*lacZ*, a transcriptional reporter of the GcrA target promoter P_{tipF} directing expression of the TipF flagellar regulator/cyclic-di-GMP receptor protein (14, 28), showed a PtsP/SpoT-dependent response similar to that with P_{ctrA}-*lacZ* and P_{mopJ}-*lacZ* (see Fig. S3C in the supplemental material).

DISCUSSION

Two concerted pathways involving the PAS domain protein MopJ (23) and the GAF domain protein PtsP are now known to promote the accumulation of the conserved cell cycle regulator CtrA in stationary phase and when *C. crescentus* cycles during exponential growth. While we previously established that MopJ acts on the components that regulate CtrA phosphorylation and stability (23), our work here revealed that PtsP signals through the (p)ppGpp synthase/hydrolase SpoT. Induction of (p)ppGpp during starvation and ectopically in nutrient-rich medium (19, 21) enhances CtrA levels while reducing DnaA synthesis and/or stability, ultimately slowing growth and cell cycle progression and inducing a G_1-phase arrest (19, 21, 29, 30).

Although the effects of (p)ppGpp on CtrA and DnaA abundance are reported to occur at the post-transcriptional level, we additionally report evidence of a transcriptional induction (directly or indirectly) of GcrA target promoters based on population-based measurements. While a specific and direct

FIG 3 PtsP regulates CtrA synthesis in stationary phase. (A and B) Promoter-probe assays of transcriptional reporters carrying a *fljM*, *sciP*, *pilA*, or *fljK* promoter fused to a promoterless *lacZ* gene in WT, Δ*mopJ* or Δ*ptsP* single mutants, the Δ*mopJ* Δ*ptsP* double mutant, and suppressor mutants Δ*mopJ ptsP*(S104P) and Δ*mopJ ptsP*(Q153P) in exponential (exp.) (A) and stationary (stat.) (B) phases. The graphs show *lacZ*-encoded β-galactosidase activities, measured in Miller units. Error bars indicate standard deviations (SD). (C and D) Immunoblot showing the steady-state levels of the major flagellin FljK, the SciP negative regulator, and the PilA structural subunit of the pilus filament in WT, Δ*mopJ* and Δ*ptsP* single mutants, the Δ*mopJ* Δ*ptsP* double mutant, and suppressor mutants Δ*mopJ ptsP*(S104P) and Δ*mopJ ptsP*(Q153P) in exponential (C) and stationary (D) phases. The steady-state levels of the MreB actin are shown as a loading control. (E) Immunoblot showing the steady-state levels of CtrA (or CtrA-M2), PtsP (or PtsPΔ*GAF*) and MreB (loading control) in various mutants in exponential and stationary phases. (F) Promoter-probe assays of transcriptional reporters carrying the *ctrA* promoter fused to a promoterless *lacZ* gene in the WT and various mutants in exponential (left) and stationary (right) growth phases. The graphs show *lacZ*-encoded β-galactosidase activities measured relative to the WT. Error bars show the SD.

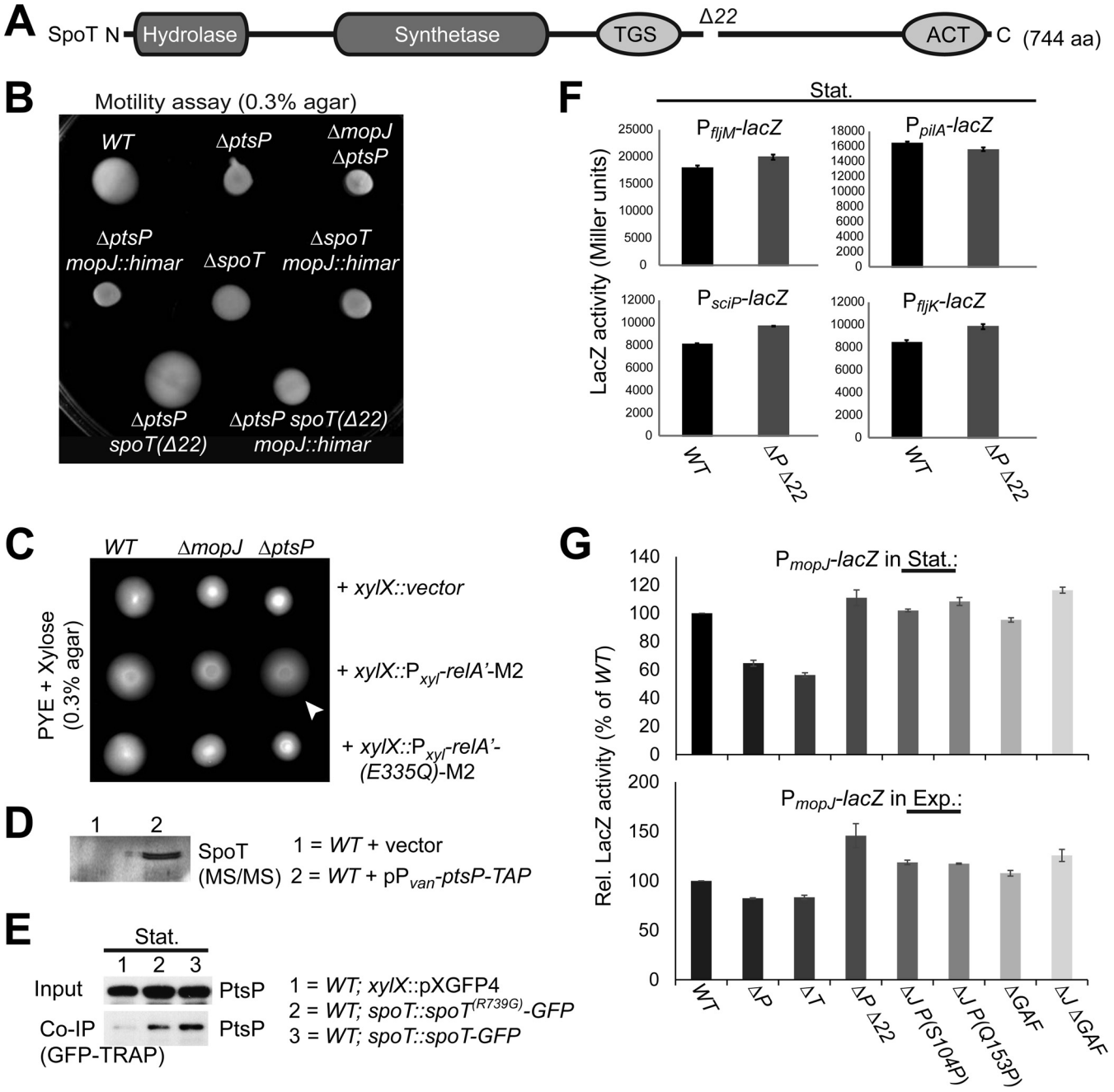

FIG 4 Genetic and physical interactions between PtsP and the (p)ppGpp synthase SpoT. (A) Domain organization of *Caulobacter* SpoT. The asterisk marks the position of the suppressor mutation. The hydrolase and synthase domains are also indicated, along with two conserved regulatory domains in the C-terminal part of SpoT. (B) Motility assay on a swarm agar plate of WT, Δ*ptsP* and Δ*spoT* single mutants, Δ*mopJ* Δ*ptsP*, Δ*ptsP mopJ::himar1*, and Δ*spoT mopJ::himar1* double mutants, the spontaneous motility suppressor of the Δ*ptsP* mutant, Δ*ptsP spoT*(Δ22), and the Δ*ptsP spoT*(Δ22) *mopJ::himar1* triple mutant. (C) Swarm agar assay with WT and Δ*mopJ* and Δ*ptsP* single mutants upon expression of the constitutive active form of *E. coli* RelA fused to the FLAG (M2) tag (RelA′-M2) in the presence of xylose. The controls harboring the inactivated form of RelA′ (RelA′-E335Q-M2) and the empty vector are also shown. The arrowhead points to the increase in motility in Δ*ptsP* cells upon (p)ppGpp production by RelA′ induction. (D) Identification of SpoT by tandem mass spectrometry (MS/MS) on a silver stained gel following tandem affinity purification (TAP) from extracts of WT cells expressing PtsP-TAP from pMT335 under the control of the P_{van} promoter. (E) Coimmunoprecipitation (Co−IP) of PtsP with green fluorescent protein (GFP)-tagged SpoT from a GFP-TRAP affinity matrix (ChromoTek GmbH, Planegg-Martinsried, Germany). Precipitated samples were probed for the presence of PtsP by immunoblotting using antibodies against PtsP. Cell lysates used as input are also shown. (F) Promoter-probe assays of transcriptional reporters carrying the *fljM*, *sciP*, *pilA*, or *fljK* promoter fused to a promoterless *lacZ* gene in WT and Δ*ptsP spoT*(Δ22) cells in stationary phase. Error bars show the standard deviations (SD). (G) Promoter-probe assays of transcriptional reporter carrying the *mopJ* promoter fused to a promoterless *lacZ* gene in WT, Δ*ptsP* and Δ*spoT* single mutants, Δ*ptsP spoT*(Δ22), Δ*mopJ ptsP*(S104P), Δ*mopJ ptsP*(Q153P) suppressor mutants, and *ptsP*Δ*GAF* and Δ*mopJ ptsP*Δ*GAF* mutants cells in stationary (top) and exponential (bottom) phases. Error bars show SD.

mechanism may underlie GcrA-dependent promoter control, it is possible that the effect of (p)ppGpp is indirect, perhaps due to an extension of the cell cycle stage when GcrA is active (Fig. 1A). In a complementary study, González and Collier (31) recently reported that loss-of-function mutations in *ptsP* partially mitigate the cell division defect of cells lacking the CcrM DNA methyltransferase (32, 33). In the absence of CcrM, GcrA targets, including the promoters of the cell division genes *ftsZ* and its regulator *mipZ*, are poorly active (14, 32), because GcrA is no longer efficiently recruited (14, 33). Our finding that PtsP and SpoT affect GcrA target promoter activity is consistent with the result that *ptsP* suppressor mutations augment *mipZ* and *ftsZ* expression, and thus *ptsP* mutations surface as suppressor mutations that enhance growth of CcrM-deficient cells (31). While the abundance and localization of PtsP do not appear to change during the cell cycle (Fig. 1F and G), PtsP is upregulated in stationary phase (Fig. 3E; see also Fig. S2C in the supplemental material). The N-terminal GAF domain seems to fulfill a critical sensory role for PtsP, because gain-of-function mutations in the GAF domain emerged here as motility suppressors of the Δ*mopJ* mutant, and as suppressors of CcrM-deficient cells in the study by González and Collier. Remarkably, mutations in *mopJ* (CCNA_00999; not identified as *mopJ* [31]), *divL* (encoding a key component of the HA relay for CtrA that is regulated by MopJ [23]), and/or *ctrA* itself can cooccur with *ptsP* mutations, reinforcing the genetic relationship between the PtsP and MopJ signaling pathways detailed here. Moreover, our observations that the activity of the *mopJ* promoter (P_{mopJ}) increased upon induction of (p)ppGpp and that P_{mopJ} is also a direct GcrA target reveal an additional layer of complexity in the intricate interplay of these two signaling pathways that affect the cell cycle and motility.

Under natural conditions, (p)ppGpp is induced during carbon, ammonium, or iron exhaustion in *Caulobacter* spp. (18), but it is also present in reduced amounts during growth in rich (peptone-yeast extract [PYE]) medium. Unlike for *E. coli*, amino acid starvation is not sufficient to induce (p)ppGpp in *Caulobacter* spp. or in several other alphaproteobacteria (27), but SpoT is required for recovery from fatty acid starvation in *C. crescentus* (34). The mechanism underlying SpoT activation for lipid starvation in *E. coli* involves an interaction of the C-terminal regulatory domain of SpoT with the acyl carrier protein (35), an essential factor for fatty acid synthesis. How SpoT is activated by other starvation conditions is less clear, but our findings raise the intriguing possibility that PtsP couples (p)ppGpp production by SpoT with carbon starvation (or other nutrient limitation in stationary phase), for example, through fluctuations in the glycolytic intermediate PEP, the phosphodonor for PtsP (36). As glutamine inhibits phosphorylation of *Sinorhizobium meliloti* PtsP *in vitro* (37), PtsP (and thus SpoT) signaling may be regulated in additional ways, for example, via the PtsN (EII) component of the alternative PTS system (PTS^{Ntr}), which directly interacts with SpoT in the betaproteobacterium *Ralstonia eutropha* (38).

MATERIALS AND METHODS

Growth conditions. *Caulobacter crescentus* NA1000 and derivatives were cultivated at 30°C in PYE rich medium or in M2 minimal salts plus 0.2% glucose (M2G) supplemented by 0.4% liquid PYE (39). *Escherichia coli* S17-1 (40) and EC100D cells (Epicentre Technologies, Madison, WI) were cultivated at 37°C in Luria broth (LB) rich medium. Agar (1.5%) was added into M2G or PYE plates, and motility was assayed on PYE plates containing 0.3% agar. Antibiotic concentrations used for *C. crescentus* included kanamycin (solid, 20 μg/ml; liquid, 5 μg/ml), tetracycline (1 μg/ml), spectinomycin (liquid, 25 μg/ml), spectinomycin-streptomycin (solid, 30 and 5 μg/ml, respectively), gentamicin (1 μg/ml), and nalidixic acid (20 μg/ml). When needed, D-xylose or sucrose was added at a 0.3% final concentration, glucose at a 0.2% final concentration, and vanillate at a 500 or 50 μM final concentration. For the experiments in stationary phase in PYE, cultures with an optical density at 600 nm (OD_{660}) of >1.4 were used, with the exception of those with motility suppressors: NA1000 Δ*mopJ ptsP*^{S104P} with an OD_{660} of ≈1.1 and NA1000 Δ*mopJ ptsP*^{Q153P} and NA1000 Δ*ptsP spoT*$^{\Delta 22}$ with an OD_{660} of ≈1.3 were used. For the experiments in stationary phase in M2G, cultures with an OD_{660} of >1.7 were used. Swarmer cell isolation, electroporation, biparental mating, and bacteriophage φCr30-mediated generalized transductions were performed as described in reference 39.

Motility suppressors of Δ*mopJ* and Δ*ptsP* mutant cells. Spontaneous mutations that suppress the motility defect of the Δ*mopJ* mutation appeared as "flares" that emanated from nonmotile colonies after approximately 3 days of incubation. Two isolates were subjected to whole-genome sequencing, and mutations in the *ptsP* gene (*ptsP*^{S104P} and *ptsP*^{Q153P}) were found. In the first one, the serine codon (TCG) at position 104 in *ptsP* was changed to one encoding proline (CCG). In the second, the glutamine codon (CAG) at position 153 in *ptsP* was changed to one encoding proline (CCG). Spontaneous mutations that suppressed the motility defect of the Δ*ptsP* mutant appeared as "flares" that emanated from the nonmotile colony after approximately 3 days of incubation. Two isolates were subjected to whole-genome sequencing, and a mutation in the *spoT* gene (*spoT*$^{\Delta 22}$) was found in one isolate, with residues 493 to 514 of the SpoT-coding sequence deleted.

Tandem affinity purification. The tandem affinity purification procedure was based on that described previously in reference 41. Briefly, when the culture (1 liter) reached an OD_{660} of 0.4 to 0.6 in the presence of 50 μM vanillate, cells were harvested by centrifugation at 6,000 × *g* for 10 min. The pellet was then washed in 50 ml of buffer I (50 mM sodium phosphate [pH 7.4], 50 mM NaCl, 1 mM EDTA) and lysed for 15 min at room temperature in 10 ml of buffer II (buffer I plus 0.5% *n*-dodecyl-β-D-maltoside, 10 mM $MgCl_2$, two protease inhibitor tablets [for 50 ml of buffer II; Complete EDTA-free; Roche], 1× Ready-Lyse lysozyme [Epicentre], 500 U of DNase I [Roche]). Cellular debris was removed by centrifugation at 7,000 × *g* for 20 min at 4°C. The supernatant was incubated for 2 h at 4°C with IgG-Sepharose beads (GE Healthcare Biosciences) that had been washed once with IPP150 buffer (10 mM Tris-HCl [pH 8], 150 mM NaCl, 0.1% NP-40). After incubation, the beads were washed at 4°C three times with 10 ml of IPP150 buffer and once with 10 ml of tobacco etch virus (TEV) protease cleavage buffer (10 mM Tris-HCl [pH 8], 150 mM NaCl, 0.1% NP-40, 0.5 mM EDTA, 1 mM dithiothreitol). The beads were then incubated overnight at 4°C with 1 ml of TEV solution (TEV cleavage buffer with 100 U of TEV protease per milliliter [Promega]) to release the tagged complex. $CaCl_2$ (3 μM) was then added to the solution. The sample with 3 ml of calmodulin-binding buffer (10 mM β-mercaptoethanol, 10 mM Tris-HCl [pH 8], 150 mM NaCl, 1 mM magnesium acetate, 1 mM imidazole, 2 mM $CaCl_2$, 0.1% NP-40) was incubated for 1 h at 4°C with calmodulin beads (GE Healthcare Biosciences) that previously had been washed once with calmodulin-binding buffer. After incubation, the beads were washed three times with 10 ml of calmodulin-binding buffer and eluted 5 times with 200 μl IPP150 calmodulin elution buffer (calmodulin-binding buffer with 2 mM EGTA instead of $CaCl_2$). The eluates were then concentrated using Amicon Ultra-4 spin columns (Ambion).

Flow cytometry. Fluorescence-activated cell sorting (FACS) was performed as described previously (33). Cells in exponential growth phase (OD_{660}, 0.3 to 0.6) or in stationary phase (diluted to obtain an OD_{660} of 0.3 to 0.6), cultivated in M2G, were fixed in ice-cold 70% ethanol solution. Fixed cells were resuspended in FACS staining buffer (pH 7.2; 10 mM Tris-HCl, 1 mM EDTA, 50 mM Na-citrate, 0.01% Triton X-100) and then

treated with RNase A (Roche) at 0.1 mg/ml for 30 min at room temperature. Cells were stained in FACS staining buffer containing 0.5 μM of SYTOX green nucleic acid stain solution (Invitrogen) and then analyzed using a BD Accuri C6 flow cytometer instrument (BD Biosciences, San Jose, CA, United States). Flow cytometry data were acquired and analyzed using the CFlow Plus v1.0.264.15 software (Accuri Cytometers Inc.). A total of 20,000 cells were analyzed from each biological sample. The forward scattering (FSC-A) and green fluorescence (FL1-A) parameters were used to estimate cell sizes and cell chromosome contents, respectively. Reported experimental values represent the averages of 3 independent experiments. The relative chromosome number was directly estimated from the FL1-A value of NA1000 cells treated with 20 μg/ml rifampin for 3 h at 30°C, as described previously (33). Rifampin treatment of cells blocks the initiation of chromosomal replication but allows ongoing rounds of replication to finish.

Cell generation time determinations. Cell growth in PYE or M2G medium was in an incubator at 30°C under agitation (190 rpm) and monitored at OD_{660}. Generation time values were extracted from the curves by using the Doubling Time application. Values represent the averages of at least 3 independent clones.

Bacterial strains, plasmids, and oligonucleotides, as well as methods for immunoblotting, coimmunoprecipitation, microscopy, and β-galactosidase assays are described in the supplemental material.

SUPPLEMENTAL MATERIAL

Supplemental material for this article may be found at http://mbio.asm.org/lookup/suppl/doi:10.1128/mBio.01415-15/-/DCSupplemental.

Figure S1, EPS file, 0.5 MB.
Figure S2, EPS file, 1.6 MB.
Figure S3, EPS file, 2.6 MB.
Text S1, DOCX file, 0.1 MB.

ACKNOWLEDGMENTS

Funding support is from SNF grant no. 31003A_143660 (to P.H.V.) and the Fondation pour des bourses d'études italo-Suisses (to S.S.).

We thank Sean Crosson (University of Chicago, USA) and Justine Collier (University of Lausanne, Switzerland) for strains. We also thank lab members Silvia Ardissone for raising the CtrA antibody, Gaël Panis for help with FACS, and Laurence Théraulaz for excellent technical assistance.

REFERENCES

1. **Guttenplan SB, Kearns DB.** 2013. Regulation of flagellar motility during biofilm formation. FEMS Microbiol Rev **37:**849–871. http://dx.doi.org/10.1111/1574-6976.12018.
2. **Skerker JM, Laub MT.** 2004. Cell-cycle progression and the generation of asymmetry in *Caulobacter crescentus*. Nat Rev Microbiol **2:**325–337. http://dx.doi.org/10.1038/nrmicro864.
3. **Quon KC, Marczynski GT, Shapiro L.** 1996. Cell cycle control by an essential bacterial two-component signal transduction protein. Cell **84:**83–93. http://dx.doi.org/10.1016/S0092-8674(00)80995-2.
4. **Sommer JM, Newton A.** 1991. Pseudoreversion analysis indicates a direct role of cell division genes in polar morphogenesis and differentiation in *Caulobacter crescentus*. Genetics **129:**623–630.
5. **Laub MT, McAdams HH, Feldblyum T, Fraser CM, Shapiro L.** 2000. Global analysis of the genetic network controlling a bacterial cell cycle. Science **290:**2144–2148. http://dx.doi.org/10.1126/science.290.5499.2144.
6. **Fiebig A, Herrou J, Fumeaux C, Radhakrishnan SK, Viollier PH, Crosson S.** 2014. A cell cycle and nutritional checkpoint controlling bacterial surface adhesion. PLoS Genet **10:**e1004101. http://dx.doi.org/10.1371/journal.pgen.1004101.
7. **Fumeaux C, Radhakrishnan SK, Ardissone S, Theraulaz L, Frandi A, Martins D, Nesper J, Abel S, Jenal U, Viollier PH.** 2014. Cell cycle transition from S-phase to G_1 in *Caulobacter* is mediated by ancestral virulence regulators. Nat Commun **5:**4081. http://dx.doi.org/10.1038/ncomms5081.
8. **Quon KC, Yang B, Domian IJ, Shapiro L, Marczynski GT.** 1998. Negative control of bacterial DNA replication by a cell cycle regulatory protein that binds at the chromosome origin. Proc Natl Acad Sci U S A **95:**120–125. http://dx.doi.org/10.1073/pnas.95.1.120.
9. **Bastedo DP, Marczynski GT.** 2009. CtrA response regulator binding to the *Caulobacter* chromosome replication origin is required during nutrient and antibiotic stress as well as during cell cycle progression. Mol Microbiol **72:**139–154. http://dx.doi.org/10.1111/j.1365-2958.2009.06630.x.
10. **Domian IJ, Quon KC, Shapiro L.** 1997. Cell type-specific phosphorylation and proteolysis of a transcriptional regulator controls the G_1-to-S transition in a bacterial cell cycle. Cell **90:**415–424. http://dx.doi.org/10.1016/S0092-8674(00)80502-4.
11. **West AH, Stock AM.** 2001. Histidine kinases and response regulator proteins in two-component signaling systems. Trends Biochem Sci **26:**369–376. http://dx.doi.org/10.1016/S0968-0004(01)01852-7.
12. **Tsokos CG, Laub MT.** 2012. Polarity and cell fate asymmetry in *Caulobacter crescentus*. Curr Opin Microbiol **15:**744–750. http://dx.doi.org/10.1016/j.mib.2012.10.011.
13. **Holtzendorff J, Hung D, Brende P, Reisenauer A, Viollier PH, McAdams HH, Shapiro L.** 2004. Oscillating global regulators control the genetic circuit driving a bacterial cell cycle. Science **304:**983–987. http://dx.doi.org/10.1126/science.1095191.
14. **Fioravanti A, Fumeaux C, Mohapatra SS, Bompard C, Brilli M, Frandi A, Castric V, Villeret V, Viollier PH, Biondi EG.** 2013. DNA binding of the cell cycle transcriptional regulator GcrA depends on N6-adenosine methylation in *Caulobacter crescentus* and other Alphaproteobacteria. PLoS Genet **9:**e1003541. http://dx.doi.org/10.1371/journal.pgen.1003541.
15. **Iniesta AA, McGrath PT, Reisenauer A, McAdams HH, Shapiro L.** 2006. A phospho-signaling pathway controls the localization and activity of a protease complex critical for bacterial cell cycle progression. Proc Natl Acad Sci U S A **103:**10935–10940. http://dx.doi.org/10.1073/pnas.0604554103.
16. **Biondi EG, Reisinger SJ, Skerker JM, Arif M, Perchuk BS, Ryan KR, Laub MT.** 2006. Regulation of the bacterial cell cycle by an integrated genetic circuit. Nature **444:**899–904. http://dx.doi.org/10.1038/nature05321.
17. **Potrykus K, Cashel M.** 2008. (p)ppGpp: still magical? Annu Rev Microbiol **62:**35–51. http://dx.doi.org/10.1146/annurev.micro.62.081307.162903.
18. **Boutte CC, Crosson S.** 2011. The complex logic of stringent response regulation in *Caulobacter crescentus*: starvation signalling in an oligotrophic environment. Mol Microbiol **80:**695–714. http://dx.doi.org/10.1111/j.1365-2958.2011.07602.x.
19. **Boutte CC, Henry JT, Crosson S.** 2012. ppGpp and polyphosphate modulate cell cycle progression in *Caulobacter crescentus*. J Bacteriol **194:**28–35. http://dx.doi.org/10.1128/JB.05932-11.
20. **Lesley JA, Shapiro L.** 2008. SpoT regulates DnaA stability and initiation of DNA replication in carbon-starved *Caulobacter crescentus*. J Bacteriol **190:**6867–6880. http://dx.doi.org/10.1128/JB.00700-08.
21. **Gonzalez D, Collier J.** 2014. Effects of (p)ppGpp on the progression of the cell cycle of *Caulobacter crescentus*. J Bacteriol **196:**2514–2525. http://dx.doi.org/10.1128/JB.01575-14.
22. **De Nisco NJ, Abo RP, Wu CM, Penterman J, Walker GC.** 2014. Global analysis of cell cycle gene expression of the legume symbiont *Sinorhizobium meliloti*. Proc Natl Acad Sci U S A **111:**3217–3224. http://dx.doi.org/10.1073/pnas.1400421111.
23. **Sanselicio S, Berge M, Theraulaz L, Radhakrishnan SK, Viollier PH.** 2015. Topological control of the *Caulobacter* cell cycle circuitry by a polarized single-domain PAS protein. Nat Commun **6:**7005. http://dx.doi.org/10.1037/ncomms8005.
24. **Henry JT, Crosson S.** 2011. Ligand-binding PAS domains in a genomic, cellular, and structural context. Annu Rev Microbiol **65:**261–286. http://dx.doi.org/10.1146/annurev-micro-121809-151631.
25. **Tchieu JH, Norris V, Edwards JS, Saier MH, Jr.** 2001. The complete phosphotransferase system in *Escherichia coli*. J Mol Microbiol Biotechnol **3:**329–346.
26. **Domian IJ, Reisenauer A, Shapiro L.** 1999. Feedback control of a master bacterial cell-cycle regulator. Proc Natl Acad Sci U S A **96:**6648–6653. http://dx.doi.org/10.1073/pnas.96.12.6648.
27. **Boutte CC, Crosson S.** 2013. Bacterial lifestyle shapes stringent response activation. Trends Microbiol **21:**174–180. http://dx.doi.org/10.1016/j.tim.2013.01.002.
28. **Davis NJ, Cohen Y, Sanselicio S, Fumeaux C, Ozaki S, Luciano J, Guerrero-Ferreira RC, Wright ER, Jenal U, Viollier PH.** 2013. De- and repolarization mechanism of flagellar morphogenesis during a bacterial

cell cycle. Genes Dev **27:**2049–2062. http://dx.doi.org/10.1101/gad.222679.113.
29. **Gorbatyuk B, Marczynski GT**. 2005. Regulated degradation of chromosome replication proteins DnaA and CtrA in *Caulobacter crescentus*. Mol Microbiol **55:**1233–1245. http://dx.doi.org/10.1111/j.1365-2958.2004.04459.x.
30. **Leslie DJ, Heinen C, Schramm FD, Thüring M, Aakre CD, Murray SM, Laub MT, Jonas K**. 2015. Nutritional control of DNA replication initiation through the proteolysis and regulated translation of DnaA. PLoS Genet **11:**e1005342. http://dx.doi.org/10.1371/journal.pgen.1005342.
31. **Gonzalez D, Collier J**. 2015. Genomic adaptations to the loss of a conserved bacterial DNA methyltransferase. mBio **6:**e00952-15. http://dx.doi.org/10.1128/mBio.00952-15.
32. **Gonzalez D, Collier J**. 2013. DNA methylation by CcrM activates the transcription of two genes required for the division of *Caulobacter crescentus*. Mol Microbiol **88:**203–218. http://dx.doi.org/10.1111/mmi.12180.
33. **Murray SM, Panis G, Fumeaux C, Viollier PH, Howard M**. 2013. Computational and genetic reduction of a cell cycle to its simplest, primordial components. PLoS Biol **11:**e1001749. http://dx.doi.org/10.1371/journal.pbio.1001749.
34. **Stott KV, Wood SM, Blair JA, Nguyen BT, Herrera A, Mora YGP, Cuajungco MP, Murray SR**. 2015. (p)ppGpp modulates cell size and the initiation of DNA replication in *Caulobacter crescentus* in response to a block in lipid biosynthesis. Microbiology **161:**553–564 http://dx.doi.org/10.1099/mic.0.000032.
35. **Battesti A, Bouveret E**. 2006. Acyl carrier protein/SpoT interaction, the switch linking SpoT-dependent stress response to fatty acid metabolism. Mol Microbiol **62:**1048–1063. http://dx.doi.org/10.1111/j.1365-2958.2006.05442.x.
36. **Pfluger K, de Lorenzo V**. 2008. Evidence of in vivo cross talk between the nitrogen-related and fructose-related branches of the carbohydrate phosphotransferase system of *Pseudomonas putida*. J Bacteriol **190:**3374–3380. http://dx.doi.org/10.1128/JB.02002-07.
37. **Goodwin RA, Gage DJ**. 2014. Biochemical characterization of a nitrogen-type phosphotransferase system reveals that enzyme EI(Ntr) integrates carbon and nitrogen signaling in *Sinorhizobium meliloti*. J Bacteriol **196:**1901–1907. http://dx.doi.org/10.1128/JB.01489-14.
38. **Karstens K, Zschiedrich CP, Bowien B, Stulke J, Gorke B**. 2014. Phosphotransferase protein EIIANtr interacts with SpoT, a key enzyme of the stringent response, in *Ralstonia eutropha* H16. Microbiology **160:**711–722. http://dx.doi.org/10.1099/mic.0.075226-0.
39. **Ely B**. 1991. Genetics of *Caulobacter crescentus*. Methods Enzymol **204:**372–384.
40. **Simon R, Priefer U, Pühler A**. 1983. A broad host range mobilization system for in vivo genetic engineering: transposon mutagenesis in gram negative bacteria. Nat Biotechnol **1:**784–790. http://dx.doi.org/10.1038/nbt1183-784.
41. **Rigaut G, Shevchenko A, Rutz B, Wilm M, Mann M, Séraphin B**. 1999. A generic protein purification method for protein complex characterization and proteome exploration. Nat Biotechnol **17:**1030–1032. http://dx.doi.org/10.1038/13732.